The Astrophysical Journal, 744:148 (9pp), 2012 January 10 doi:10.1088/0004-637X/744/2/148

CANDELS: CONSTRAINING THE AGN–MERGER CONNECTION WITH HOST MORPHOLOGIES AT $z \sim 2$

Dale D. Kocevski[1], S. M. Faber[1], Mark Mozena[1], Anton M. Koekemoer[2], Kirpal Nandra[3], Cyprian Rangel[4], Elise S. Laird[4], Marcella Brusa[3], Stijn Wuyts[3], Jonathan R. Trump[1], David C. Koo[1], Rachel S. Somerville[2,5], Eric F. Bell[6], Jennifer M. Lotz[2], David M. Alexander[7], Frederic Bournaud[8], Christopher J. Conselice[9], Tomas Dahlen[2], Avishai Dekel[10], Jennifer L. Donley[2], James S. Dunlop[11], Alexis Finoguenov[3,12], Antonis Georgakakis[13], Mauro Giavalisco[14], Yicheng Guo[14], Norman A. Grogin[2], Nimish P. Hathi[15], Stéphanie Juneau[16], Jeyhan S. Kartaltepe[17], Ray A. Lucas[2], Elizabeth J. McGrath[1], Daniel H. McIntosh[18], Bahram Mobasher[19], Aday R. Robaina[20], David Rosario[3], Amber N. Straughn[21], Arjen van der Wel[22], and Carolin Villforth[2]

[1] University of California Observatories/Lick Observatory, University of California, Santa Cruz, CA 95064, USA; kocevski@ucolick.org
[2] Space Telescope Science Institute, Baltimore, MD 21218, USA
[3] Max-Planck-Institut für extraterrestrische Physik, D-85748 Garching, Germany
[4] Astrophysics Group, Imperial College London, London, SW7 2AZ, UK
[5] Physics and Astronomy Department, Rutgers University, Piscataway, NJ 08854, USA
[6] Department of Astronomy, University of Michigan, Ann Arbor, MI 48109, USA
[7] Department of Physics, Durham University, Durham DH1 3LE, UK
[8] CEA, IRFU, SAp & Laboratoire AIM Paris-Saclay, F-91191 Gif-sur-Yvette, France
[9] Centre for Astronomy and Particle Theory, University of Nottingham, Nottingham, NG7 2RD, UK
[10] Racah Institute of Physics, The Hebrew University of Jerusalem, Jerusalem 91904, Israel
[11] Center for Space Science Technology, University of Maryland, Baltimore County, Baltimore, MD
[12] Institute for Astronomy, University of Edinburgh, Royal Observatory, Edinburgh EH9 3HJ, UK
[13] National Observatory of Athens, V. Paulou and I. Metaxa, 11532, Greece
[14] Department of Astronomy, University of Massachusetts, Amherst, MA 01003, USA
[15] The Observatoires of the Carnegie Institution of Washington, Pasadena, CA 91101, USA
[16] Steward Observatory, University of Arizona, Tucson, AZ 85721, USA
[17] NOAO-Tucson, Tucson, AZ 85719, USA
[18] University of Missouri-Kansas City, Department of Physics, Kansas City, MO 64110, USA
[19] Department of Physics and Astronomy, University of California, Riverside, CA 92521, USA
[20] Institut de Ciencies del Cosmos, ICC-UB, IEEC, E-08028, Barcelona, Spain
[21] NASA's Goddard Space Flight Center, Laboratory for Observational Cosmology, Greenbelt, MD 20771
[22] Max-Planck Institut für Astronomie, D-69117, Heidelberg, Germany
Received 2011 June 21; accepted 2011 September 20; published 2011 December 22

ABSTRACT

Using *Hubble Space Telescope*/WFC3 imaging taken as part of the Cosmic Assembly Near-infrared Deep Extragalactic Legacy Survey, we examine the role that major galaxy mergers play in triggering active galactic nucleus (AGN) activity at $z \sim 2$. Our sample consists of 72 moderate-luminosity ($L_X \sim 10^{42-44}$ erg s^{-1}) AGNs at $1.5 < z < 2.5$ that are selected using the 4 Ms *Chandra* observations in the Chandra Deep Field South, the deepest X-ray observations to date. Employing visual classifications, we have analyzed the rest-frame optical morphologies of the AGN host galaxies and compared them to a mass-matched control sample of 216 non-active galaxies at the same redshift. We find that most of the AGNs reside in disk galaxies ($51.4^{+5.8}_{-5.9}$%), while a smaller percentage are found in spheroids ($27.8^{+5.8}_{-4.6}$%). Roughly $16.7^{+5.3}_{-3.5}$% of the AGN hosts have highly disturbed morphologies and appear to be involved in a major merger or interaction, while most of the hosts ($55.6^{+5.6}_{-5.9}$%) appear relatively relaxed and undisturbed. These fractions are statistically consistent with the fraction of control galaxies that show similar morphological disturbances. These results suggest that the hosts of moderate-luminosity AGNs are no more likely to be involved in an ongoing merger or interaction relative to non-active galaxies of similar mass at $z \sim 2$. The high disk fraction observed among the AGN hosts also appears to be at odds with predictions that merger-driven accretion should be the dominant AGN fueling mode at $z \sim 2$, even at moderate X-ray luminosities. Although we cannot rule out that minor mergers are responsible for triggering these systems, the presence of a large population of relatively undisturbed disk-like hosts suggests that the stochastic accretion of gas plays a greater role in fueling AGN activity at $z \sim 2$ than previously thought.

Key words: galaxies: active – galaxies: evolution – X-rays: galaxies

Online-only material: color figures

1. INTRODUCTION

Although it has been established that supermassive black holes (SMBHs) lie at the center of most, if not all, massive galaxies (Magorrian et al. 1998), the primary mechanism that turns quiescent black holes into active galactic nuclei (AGNs) is still being debated. Galaxy mergers have long been espoused as a possible fueling mechanism given their effectiveness in dissipating angular momentum and funneling gas to the center of galaxies (Barnes & Hernquist 1991; Mihos & Hernquist 1996). This can drive both accretion onto the SMBH and growth of the stellar bulge, which would help explain the tight correlations observed between the two (e.g., Gebhardt et al. 2000; Ferrarese & Merritt 2000; Marconi & Hunt 2003;

Häring & Rix 2004). In fact, recent galaxy merger simulations that incorporate a prescription for self-regulated black hole growth have successfully reproduced many observed properties of AGNs and their host galaxies. This includes the correlation between SMBH mass and bulge velocity dispersion (Di Matteo et al. 2007; Robertson et al. 2006), the quasar luminosity function (Hopkins et al. 2005, 2006b), and the luminosity function of post-quenched red galaxies (Hopkins et al. 2006a). Such simulations have shown that, when coupled with recent AGN feedback scenarios, major galaxy mergers provide an attractive mechanism to both trigger AGN activity and help explain the coevolution observed between SMBHs and their hosts (Hopkins et al. 2008).

Thus far, however, efforts to detect an AGN–merger connection have produced mixed results. At low redshifts luminous quasi-stellar objects (QSOs) have long been tied to ongoing or past merger activity (Stockton 1982; Canalizo & Stockton 2001; Bennert et al. 2008). However Dunlop et al. (2003) find that QSOs at $z \sim 0.2$ are no more likely to exhibit structural disturbances when compared to a control sample of similar non-active galaxies. At higher redshifts, several studies have used the resolving power of the *Hubble Space Telescope* (*HST*) to examine the host morphologies of X-ray-selected AGNs out to $z \sim 1.3$. Grogin et al. (2005) and Pierce et al. (2007), using data from the Great Observatories Origins Deep Survey (GOODS; Giavalisco et al. 2004) and the All-wavelength Extended Groth strip International Survey (AEGIS; Davis et al. 2007), respectively, find that host galaxies at $z \sim 1$ do not show disturbances or interaction signatures more often than their quiescent counterparts (see also Sánchez et al. 2004). More recently, Gabor et al. (2009) and Cisternas et al. (2011) examined the host morphologies of AGNs selected in the Cosmic Evolution Survey (COSMOS; Scoville et al. 2007) and report that the disturbed fraction among active and quiescent galaxies at $z \sim 1$ is not significantly different. Instead they find that a majority of AGNs at this redshift are hosted by disk galaxies that do not show strong distortions. Schawinski et al. (2011) recently extended this work to $z \sim 2$ by examining the light profiles of a relatively small number of AGNs in a portion of the GOODS-S field. They report that a majority of host galaxies at this redshift have morphologies best fit by low Sérsic indices indicative of disk-dominated galaxies and suggest that the bulk of SMBH growth since $z \sim 2$ must be driven by secular processes and not major mergers. However, this study did not examine the frequency of minor morphological disturbances, which could be indicative of past interactions, nor did it compare the morphologies of the AGN hosts against a true mass-matched control sample of non-active galaxies.

If there is a redshift at which the primary fueling mechanism of AGN transitions from secular processes to major mergers, surveys of high-redshift AGNs have yet to observe it. In this study, we extend the search for an AGN–merger connection for the first time to $z \sim 2$, the peak in the accretion history of the universe. To do this we combine high-resolution near-infrared imaging taken with *HST*/WFC3 as part of the Cosmic Assembly Near-infrared Deep Extragalactic Legacy Survey (CANDELS; Grogin et al. 2011; Koekemoer et al. 2011) with the 4 Ms *Chandra* observations of the Chandra Deep Field South (CDF-S; Xue et al. 2011), the deepest X-ray observations obtained to date. While *HST*/ACS observations have characterized the rest-frame ultraviolet structure of galaxies at $z > 1.5$ (e.g., Jahnke et al. 2004), *HST*/WFC3 observations move beyond the Balmer break ($\lambda_{\rm rest} \geqslant 4000$ Å) and hence probe the light from stars that dominate a galaxy's mass budget. This allows us to assess the rest-frame optical morphologies and true stellar structure of a large sample of AGN hosts at $z \sim 2$ for the first time. Furthermore, the increased depth of the 4 Ms data set over previous *Chandra* observations in the CDF-S provides greater sensitivity to more obscured (and hence fainter) AGNs that may have been missed in previous studies.

In this study, we report on the visual classification of galaxies hosting X-ray-selected AGNs in the CDF-S using *HST*/WFC3 imaging in the *H* band. We examine whether AGN hosts exhibit an enhancement of merger or interaction signatures relative to a mass-matched control sample at the same redshift. Our analysis is presented in the following manner: Section 2 describes the X-ray and near-infrared data used for the study, Section 3 discusses the AGN sample selection, Section 4 details the morphological classification scheme, and Section 5 presents our results. Finally, our findings and conclusions are summarized in Section 6. When necessary the following cosmological parameters are used: $H_0 = 70\,{\rm km\,s^{-1}\,Mpc^{-1}}$; $\Omega_{\rm tot}, \Omega_\Lambda, \Omega_{\rm m} = 1, 0.3, 0.7$.

2. OBSERVATIONS AND DATA DESCRIPTION

2.1. Near-infrared Imaging

The near-infrared imaging used for this study consists of WFC3/IR observations of the GOODS-S field in the F125W (*J*) and F160W (*H*) bands obtained as part of the Early Release Science program (ERS; Windhorst et al. 2011) and the ongoing CANDELS Multi-Cycle Treasury Program. The ERS data set consists of 10 WFC3/IR tiles with exposure times of 5000s (each bands) covering the northern $10' \times 4'$ region of the GOODS-South field. The CANDELS data set consists of 15 WFC3/IR tiles covering the central $\sim 10' \times 7'$ region just south of and adjacent to the ERS imaging. At the time of writing, each tile in the CANDELS data set has a total exposure time of 3000 s in both the *J* and *H* bands.

The publicly available ERS data and the CANDELS imaging were reduced as described in Koekemoer et al. (2011). Due to the difference in the exposure times of the observations, they were combined into separate mosaics with matching pixel scales of $0\farcs06$ pixel^{-1} using MultiDrizzle (Koekemoer et al. 2002). From these mosaics we produced an *H*-band-selected catalog of objects in each region using the SExtractor software (Bertin & Arnouts 1996). Further details of the CANDELS observations and data reduction can be found in Grogin et al. (2011) and Koekemoer et al. (2011).

2.2. X-Ray Observations

The 4 Ms *Chandra* imaging of the CDF-S was obtained in 54 observations (ObsIDs) over the course of three *Chandra* observing cycles in 2000, 2007, and 2010 using the Advanced CCD Imaging Spectrometer imaging array (ACIS-I; Garmire et al. 2003). The data were reduced using CIAO v4.2 according to the basic procedure described in Laird et al. (2009). Before combining the observations (and differing from Laird et al.), the astrometry of each ObsID was registered to that of the GOODS-MUSYC survey (Gawiser et al. 2006) by matching the positions of bright X-ray sources to *H*-band-selected sources, using the tool `reproject_aspect`. Source detection was carried out according to the method described in Laird et al. (2009). A total of 569 sources were detected to a Poisson probability limit (i.e., the *wavdetect* false-positive threshold) of 4e−6.

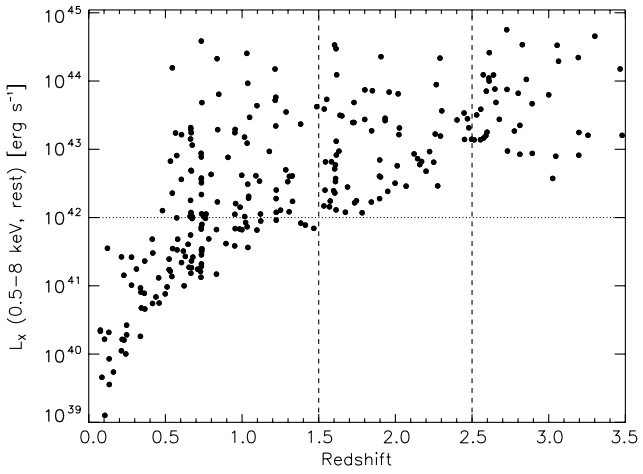

Figure 1. Redshift vs. rest-frame X-ray luminosity (0.5–8 keV) for sources detected in the 4 Ms observations of the CDF-S and which fall in the CANDELS and ERS *H*-band imaging. The vertical lines denote the target redshift range of $1.5 < z < 2.5$. The dotted horizontal line denotes a luminosity of $L_X = 10^{42}$ erg s^{-1}, the maximum X-ray luminosity attributable to starburst galaxies.

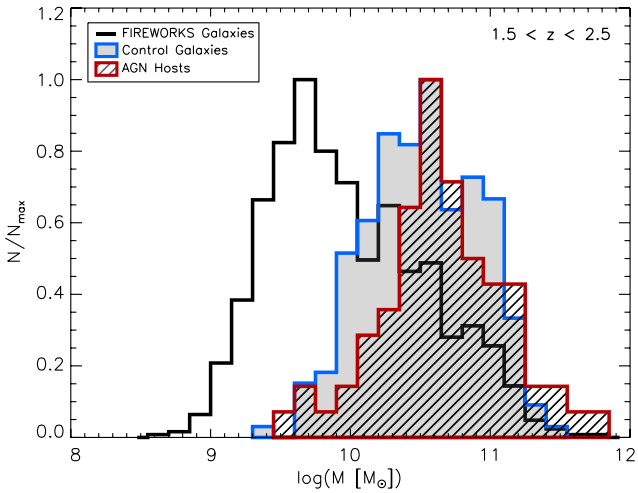

Figure 2. Mass distribution of FIREWORKS galaxies in GOODS-S with $K_s < 24.3$ AB (black) and AGN hosts (red) in the redshift range $1.5 < z < 2.5$. The distribution of our mass-matched control sample of non-active galaxies is shown in blue.

(A color version of this figure is available in the online journal.)

3. SAMPLE SELECTION

Our AGN selection is based on X-ray detections in the *Chandra* 4 Ms CDF-S observations. The power of this data set to detect AGNs at $z \sim 2$ stems from its depth and the fact that at such redshifts hard X-ray emission (∼4–5 keV) is shifted into the *Chandra* sensitivity window, which peaks at 1.5 keV, potentially allowing us to detect even heavily obscured SMBHs. At the target redshift of $z \sim 2$, the luminosity limit of these observations is roughly $L_X \sim 10^{42}$ erg s^{-1}, the maximum X-ray luminosity thought to be attributable to star formation processes (Bauer et al. 2002). This allows us to probe the entire population of moderate-luminosity AGNs at high redshifts for the first time, while ensuring that the sample is not significantly contaminated by star-forming galaxies without active nuclei.

To identify *H*-band counterparts to the X-ray sources we employed a maximum likelihood technique introduced by Sutherland & Saunders (1992) and described in Brusa et al. (2005). A total of 350/569 X-ray sources in the 4 Ms catalog fall in the area covered by the ERS and CANDELS imaging. Of these, 322 were reliably matched to an *H*-band-detected object. Four spurious associations are expected among these matches. Redshifts for the matched hosts were obtained from a variety of publicly available spectroscopic redshift catalogs (the bulk of these redshifts come from Silverman et al. 2010) and the photometric redshifts in the FIREWORKS catalog (Wuyts et al. 2008). The latter includes photometric redshift information for galaxies with $K_s < 24.3$ AB plus detections in at least four additional bands.

Using this combination of redshifts, we find 72 X-ray sources in the target redshift range of $1.5 < z < 2.5$, of which 22 are new detections not found in the shallower 2 Ms observations of the CDF-S (Luo et al. 2008). The redshift–luminosity distribution of these sources is shown in Figure 1. The sample has a median luminosity of 7.9×10^{42} erg s^{-1} in the 0.5–8 keV band (rest frame). Five sources have luminosities in excess of 10^{44} erg s^{-1}, while the faintest source has a luminosity of 1.2×10^{42} erg s^{-1}. Of the 72 *H*-band counterparts, 22 fall within the ERS region, while 50 are located in the CANDELS region. These 72 galaxies comprise the primary sample of AGN hosts studied in this analysis.

3.1. Mass-matched Control Sample

To properly compare the morphologies of the AGN hosts to similar non-active galaxies, we constructed a control sample consisting of galaxies with masses similar to those of the AGN hosts. Masses for both the active and non-active populations were obtained from the FIREWORKS catalog, where they were estimated by modeling each galaxy's observed spectral energy distribution (SED) with Bruzual & Charlot (2003) stellar population synthesis models. Non-thermal nuclear emission has previously been shown to not significantly contaminate the rest-frame optical and infrared emission of galaxies hosting moderate-luminosity AGNs such as those in our sample (e.g., Barger et al. 2005; Bundy et al. 2008). An examination of the AGN host SEDs confirms this finding for >90% of the sample. Therefore, we proceed under the assumption that the FIREWORKS-derived redshifts and masses for the bulk of the AGN sample are not systematically biased compared to the control sample.

For each AGN host, we randomly selected three unique, non-active galaxies from the FIREWORKS catalog whose masses are within a factor of two of the AGN host mass (i.e., $M_{AGN}/2 \leqslant M_{gal} \leqslant 2M_{AGN}$). Because of the difference in depth between the ERS and CANDELS observations, the control sample is selected separately for AGNs in each region, using only non-active galaxies in the corresponding region. The number of control galaxies was restricted to three per AGN due to the limited number of massive galaxies available in each field, especially the smaller ERS region.

Constructing a mass-matched control sample for this analysis is vital, as the bulk of the galaxy population at $z \sim 2$ is substantially less massive than the AGN host galaxies. This can be seen in Figure 2, which shows the mass distribution for all K_s-selected FIREWORKS galaxies (with $K_s < 24.3$ AB) in the redshift range $1.5 < z < 2.5$, as well as the masses of the AGN hosts and their corresponding control galaxies. Without taking mass into consideration, any control sample selected at $z \sim 2$ would be dominated by the low-mass population, which is predominantly composed of spiral and irregular galaxies, potentially biasing any morphological comparison.

4. VISUAL CLASSIFICATION

To determine whether the AGN host galaxies exhibit merger or interaction signatures more often than non-active galaxies of similar mass, we have visually classified the morphologies of both populations. Compared to more automated classification techniques, this type of visual inspection allows us to better pick up low surface brightness features and faint signatures of past interactions that can be missed using quantitative measures such as concentration and asymmetry (Kartaltepe et al. 2010). Classifiers were asked to determine the predominant morphological type of each galaxy and the degree to which it was disturbed. These inspections were performed blind (i.e., the AGN hosts and control galaxies were mixed) and done primarily in the *H* band, although classifiers were also given supplemental *V*-, *z*-, and *J*-band images of each galaxy in order to provide additional color information. The inspectors had access to FITS images in all four bands so as to manipulate the contrast and stretch of an image if needed. Because of the difference in depth of the ERS and CANDELS imaging, the classifications were carried out separately for the subsamples in each region.

The classification of each galaxy was split into two categories, with the first being a general morphological classification and the second a disturbance classification. For the former, inspectors were asked to choose among the following broad morphologies: *Disk, Spheroid, Irregular/Peculiar, Point-like*. Classifiers were allowed to choose as many as were applicable to a given galaxy. For example, a spiral galaxy with a substantial bulge would be classified as having both a disk and spheroid component.

The second category is meant to gauge the degree to which a galaxy is distorted or disturbed, presumably as a result of a recent interaction. The disturbance classes within this category were designed to pick up not only major mergers, but also weak interactions that may lead to only minor disturbances or asymmetries, as well as faint signatures of past merger activity. Classifiers were asked to choose one of the following disturbance classes.

1. *Merger.* Highly disturbed with multiple nuclei and/or strong distortions in a single coalescing system.
2. *Interaction.* Two distinct galaxies showing distortions and interaction features such as tidal arms.
3. *Distorted.* Single asymmetric or distorted galaxy with no visible interacting companion.
4. *Double Nuclei.* Multiple nuclei in a single coalesced system.
5. *Close Pair.* Near-neighbor pair in which both are undisturbed.
6. *Undisturbed.* None of the above.

While the *Merger* and *Interaction* classes together identify galaxies in the various stages of a highly disruptive interaction, the *Distorted* class is meant to flag more subtle signatures of minor interactions where the companion galaxy may not be visible. To improve our statistics, we have grouped several of the interaction classes into the following categories according to the severity of the observed disturbance.

1. *Disturbed I.* Highly disturbed systems. Includes galaxies in the *Merger* and *Interaction* classes.
2. *Disturbed II.* High to moderately disturbed systems. Includes all galaxies in the *Disturbed I* class, as well as systems with distorted or asymmetric morphologies (those in the *Distorted* class), and galaxies with *Double Nuclei*.
3. *Companion.* Includes all galaxies that have a neighbor within 1.″5 (12 kpc projected at $z \sim 2$). This includes all galaxies in the *Close Pair* class.

Each galaxy in the sample of 72 AGN hosts and 216 control galaxies was examined by 12 independent classifiers. The individual classifications were combined on a galaxy-by-galaxy basis using the consensus of the group. For example, a galaxy was assigned a morphological classification only if a majority (greater than half) of the inspectors agreed that that morphological component was present. Multiple morphological classifications per galaxy were possible. Since the disturbance classes are mutually exclusive, disturbance classifications were based on the class most often chosen for a given galaxy. In cases where the inspectors were evenly split, the galaxy was assigned the more disturbed interpretation. For example, a galaxy flagged as an *Interaction* and as *Disturbed* by an equal number of inspectors would be assigned the *Interaction* class. These combined classifications were then used to calculate the fraction of AGNs and control galaxies with a given morphology or disturbance class.

Further details on the CANDELS visual classification system, including how well the visual morphologies compare against quantitative morphology measures, can be found in J. S. Kartaltepe et al. (2011, in preparation). A particular concern for the AGN host galaxies is the possibility that nuclear point-source emission may mimic a central bulge component. We tested for this using parametric Sérsic (1968) fits to the surface brightness profiles of the AGN hosts (A. van der Wel et al. 2011, in preparation). The fits were done using the GALFIT package (Peng et al. 2002) and the GALAPAGOS wrapper. In general, we find broad agreement between the resulting best-fit Sérsic indices, *n*, and the visual morphologies. Only a handful of sources show signs of point-source contamination, as evidenced by best-fit Sérsic profiles that are steeper than a de Vaucouleurs profile ($n > 4$; de Vaucouleurs 1948). These sources were predominantly the most luminous AGNs in our sample and were easily identified visually as extended spheroids, despite the added nuclear emission. For these reasons we do not believe that point-source contamination has biased or strongly affecting the visual classification of the bulk of the AGN host sample.

5. RESULTS

Sample WFC3 *H*-band images of AGN host galaxies that exhibit a range of morphologies and disturbances are shown in Figure 3, while the combined results of the visual analysis of the AGN hosts and control galaxies are shown in Figure 4 and listed in Table 1. In the following sections we first present the morphological breakdown of these galaxies and later discuss the frequency of disturbances observed among them.

A brief note regarding nomenclature: in the following sections the term *disks* (or *all disks*) refers to all galaxies with a visible disk, including those with and without a discernible central bulge. We will use the term *pure disks* to refer to disk-like galaxies where no bulge is discernible. On the other hand, the term *spheroids* (or *pure spheroids*) refers to spheroidal galaxies with no discernible disk component. At times we will use the term *all spheroids* to refer to both pure spheroids and the bulge component of galaxies with a visible disk.

5.1. Host Morphologies

Shown on the left side of Figure 4 is the fraction of AGN hosts and control galaxies that were classified as having disk,

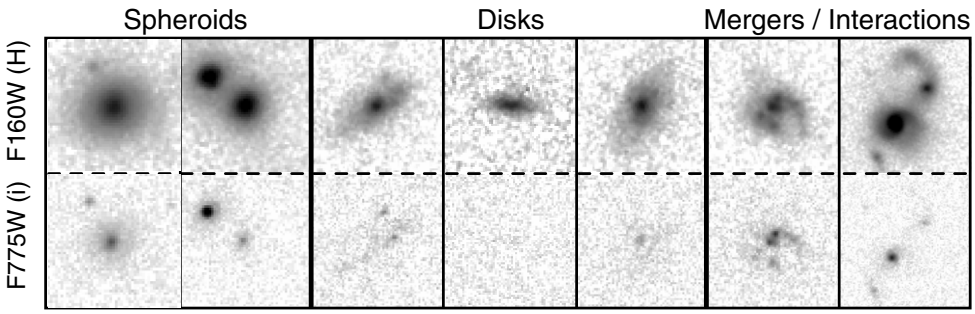

Figure 3. Examples of AGN host galaxies that were classified as having spheroid and disk morphologies, as well as two galaxies experiencing disruptive interactions. Thumbnails on the top row are WFC3/IR images taken in the F160W (*H*) band (rest-frame optical), while those on the bottom row are from ACS/WFC in the F775W (*i*) band (rest-frame ultraviolet). These images demonstrate that accurately classifying the morphology of these galaxies at $z \sim 2$ requires *H*-band imaging.

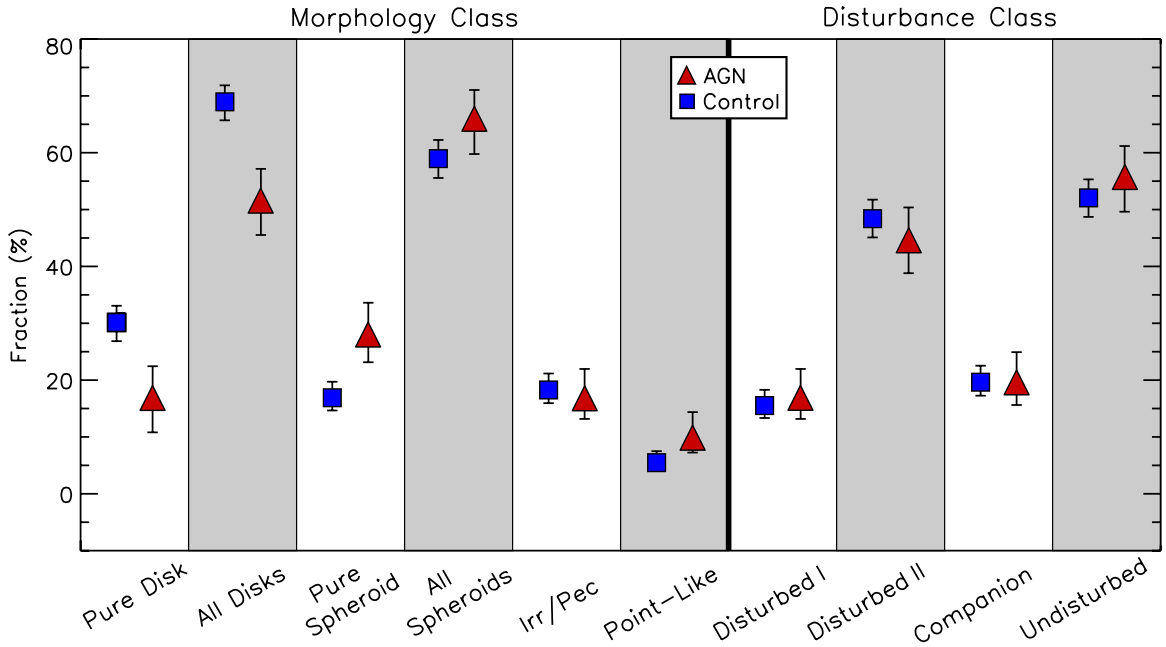

Figure 4. Fraction of AGN hosts (red triangles) and control galaxies (blue squares) at $1.5 < z < 2.5$ assigned to various morphological and disturbance classes. The *Pure Disk* class includes only disks without a central bulge. The *Pure Disk* class is a subsample of the *All Disks* class, which includes disks with and without a central bulge. Similarly, the *Pure Spheroid* class includes only spheroids with no discernible disk component. The *All Spheroids* class includes both *Pure Spheroids* and disk galaxies with a central bulge. The *Disturbed I* class is limited to heavily disturbed galaxies in a clear merger or interaction. The *Disturbed II* class includes galaxies in the *Disturbed I* class, as well as those showing even minor asymmetries in their morphologies. See the text for details.

(A color version of this figure is available in the online journal.)

Table 1
Visual Classification Results

Classification	AGN Hosts	Control Galaxies	AGN $L_X < 10^{43}$ erg s^{-1}	AGN $L_X > 10^{43}$ erg s^{-1}
Pure disk	$16.7^{+5.3}_{-3.5}$ %	$30.1^{+3.3}_{-2.9}$ %	$21.0^{+8.0}_{-5.1}$ %	$12.5^{+8.2}_{-3.7}$ %
All disks	$51.4^{+5.8}_{-5.9}$ %	$69.0^{+2.9}_{-3.3}$ %	$68.4^{+6.5}_{-8.3}$ %	$34.4^{+9.1}_{-7.3}$ %
Pure spheroid	$27.8^{+5.8}_{-4.6}$ %	$16.9^{+2.8}_{-2.2}$ %	$18.4^{+7.9}_{-4.7}$ %	$40.6^{+9.0}_{-7.9}$ %
All spheroids	$62.5^{+5.3}_{-6.0}$ %	$55.7^{+3.3}_{-3.4}$ %	$65.8^{+6.7}_{-8.3}$ %	$62.5^{+7.5}_{-9.1}$ %
Irregular	$16.7^{+5.3}_{-3.5}$ %	$18.2^{+2.9}_{-2.3}$ %	$21.0^{+8.0}_{-5.1}$ %	$06.3^{+7.3}_{-2.1}$ %
Point-like	$09.7^{+4.7}_{-2.5}$ %	$05.5^{+2.0}_{-1.2}$ %	$02.6^{+5.6}_{-0.8}$ %	$18.8^{+8.7}_{-5.0}$ %
Disturbed I	$16.7^{+5.3}_{-3.5}$ %	$15.5^{+2.8}_{-2.2}$ %	$15.8^{+7.7}_{-4.2}$ %	$18.8^{+8.7}_{-5.0}$ %
Disturbed II	$44.4^{+5.9}_{-5.6}$ %	$48.4^{+3.4}_{-3.4}$ %	$36.8^{+8.3}_{-7.0}$ %	$53.1^{+8.4}_{-8.8}$ %
Companion	$19.4^{+5.5}_{-3.8}$ %	$19.6^{+3.0}_{-2.4}$ %	$18.4^{+7.9}_{-4.7}$ %	$21.9^{+8.9}_{-5.6}$ %
Undisturbed	$55.6^{+5.6}_{-5.9}$ %	$52.1^{+3.3}_{-3.4}$ %	$63.2^{+7.0}_{-8.3}$ %	$46.9^{+8.7}_{-8.4}$ %

Notes. The *Pure Disk* and *Pure Spheroid* classes are included in the *All Disks* and *All Spheroids* classes, respectively. Likewise, the *Disturbed I* class is a subset of the *Disturbed II* class.

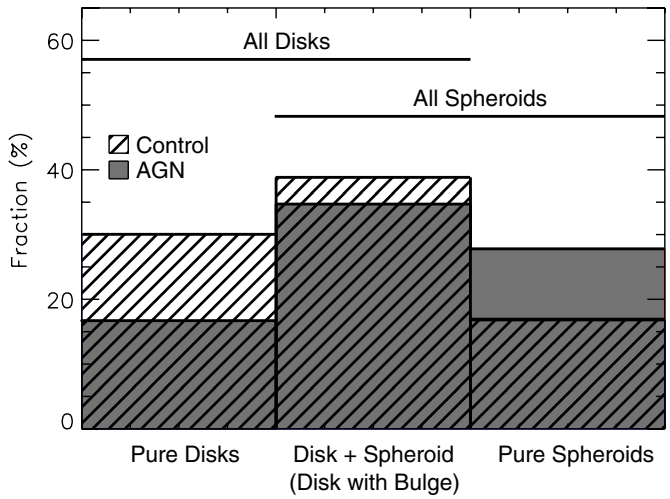

Figure 5. Fraction of AGN hosts and control galaxies at $1.5 < z < 2.5$ classified as bulgeless pure disks, disks with central bulges and pure spheroids. The AGNs tend to favor more spheroid-dominated hosts as they show an excess of pure spheroid morphologies relative to the control sample and a deficit of pure disk morphologies.

spheroid, point-like, or irregular morphologies. The error bars on each fraction reflect the 68.3% binomial confidence limits given the number of sources in each category, calculated using the method of Cameron (2011). For the disk fraction, we show both the fraction of AGNs found in pure disks (i.e., those with no discernible bulge) and the fraction hosted by any disky galaxy (i.e., disks with and without a discernible bulge).

If AGN activity at $z \sim 2$ is triggered predominantly by major mergers, we might expect an increased incidence of irregular morphologies among the AGN hosts. Instead, we find the irregular fraction to be relatively low ($16.7^{+5.3}_{-3.5}$%) and consistent with the fraction observed among the control sample ($18.2^{+2.9}_{-2.3}$%). This is the first indication that AGNs are not found in substantially disturbed galaxies more often than their non-active counterparts at this redshift. In fact, a high fraction of the AGNs are found in galaxies with a visible disk, a component which is unlikely to have survived a major merger in the recent past. We find disks to be the most common single morphology assigned to the AGN hosts, making up $51.4^{+5.8}_{-5.9}$% of the entire sample. Two-thirds of these galaxies (67.6%) also exhibit a prominent bulge component, while 32.4% of the disk galaxies show no discernible central bulge. Of the remaining hosts, pure spheroids comprise $27.8^{+5.8}_{-4.6}$% of the entire sample, while point-like sources constitute $9.7^{+4.7}_{-2.5}$%.

Despite the prevalence of disks among the AGN hosts, we find that the active galaxies are more often associated with spheroid morphologies than their non-active counterparts. Pure spheroids make up $27.8^{+5.8}_{-4.6}$% of the AGN hosts versus only $16.9^{+2.8}_{-2.2}$% of the massive control galaxies. Disks, on the other hand, are more common among the control sample, comprising $69.0^{+2.9}_{-3.3}$% of the non-active galaxies, but only $51.4^{+5.8}_{-5.9}$% of the AGN hosts. The smaller disk fraction among the active galaxies compared to the control galaxies is significant at the 99.6% level, assuming a binomial error distribution.

The fact that the AGNs tend to favor more spheroid-dominated hosts is further illustrated in Figure 5, where we show the fraction of active and control galaxies classified as pure disks, disks with central bulges and pure spheroids. The AGN host morphologies are skewed toward more spheroid-dominated systems as they show an excess of pure spheroid morphologies relative to the control sample and a deficit of pure disk morphologies. We find that bulgeless, pure disks constitute $30.1^{+3.3}_{-2.9}$% of the control population while making up only $16.7^{+5.3}_{-3.5}$% of the AGN host galaxies. These findings suggest that the trend observed at lower redshifts, that AGN hosts are more spheroid-dominated relative to similarly massive non-active galaxies (e.g., Grogin et al. 2005; Pierce et al. 2007), continues to some extent out to $z \sim 2$.

Lastly, we have considered the possibility that host morphology, and hence triggering mechanisms, vary systematically with X-ray luminosity. To investigate this, we have examined the morphologies of active galaxies with X-ray luminosities above and below $L_X = 10^{43}$ erg s^{-1}. These subsamples include 32 and 40 AGNs, respectively, out of the full sample of 72 at $z \sim 2$. The morphological breakdown of these subsamples is listed in Table 1. We find no increase in the irregular fraction among the more luminous AGNs, but we do observe a dramatic reversal in the spheroid and disk fractions: spheroids constitute $40.6^{+9.0}_{-7.9}$% of the galaxies hosting the more X-ray luminous AGNs, while the disk fraction drops to $34.4^{+9.1}_{-7.3}$%. This is compared to a spheroid and disk fraction of $18.4^{+7.9}_{-4.7}$% and $68.4^{+6.5}_{-8.3}$%, respectively, for the lower luminosity sample. This finding agrees with local host properties, where luminous AGNs and QSOs tend to be more often associated with early-type hosts (Kauffmann et al. 2003).

5.2. Interaction Signatures

The fraction of active and non-active galaxies that exhibit various levels of disturbance in their morphologies is shown on the right side of Figure 4 and the bottom part of Table 1. We find that $16.7^{+5.3}_{-3.5}$% of the AGN hosts are involved in highly disruptive mergers or interactions and fall in the *Disturbed I* category. This percentage is statistically no different than the fraction of similarly disturbed non-active galaxies ($15.5^{+2.8}_{-2.2}$%). If we include galaxies showing minor asymmetries in their morphologies and those with double nuclei (i.e., *Disturbed II* systems), the fraction of disturbed active galaxies increases to $44.4^{+5.9}_{-5.6}$%. This is below the percentage of control galaxies that fall in the same category ($48.4^{+3.4}_{-3.4}$%), but the fractions are again statistically equivalent. In fact, for all of the distortion classes we considered, the properties of the AGN hosts are not significantly different than the non-active sample. This includes the fraction showing clear merger and interaction signatures (see Table 1), those with only a minor asymmetry in their morphology ($30.6^{+4.9}_{-5.9}$% for AGNs versus $32.9^{+3.0}_{-3.3}$% for the control sample, respectively), and the frequency of companions within 1.″5 (12 kpc projected; $19.4^{+5.5}_{-3.8}$% versus $19.6^{+3.0}_{-2.4}$%).

The most common disturbance class assigned to both the AGN hosts and control galaxies is *Undisturbed*, making up $55.6^{+5.6}_{-5.9}$% and $52.1^{+3.3}_{-3.4}$% of each population, respectively. This suggests that a majority of the AGNs at $z \sim 2$ reside in relatively relaxed galaxies that do not show even minor disturbances in our *H*-band imaging. Significantly, these results do not change when we limit our analysis to the more luminous AGNs in the sample: the *Undisturbed* fraction is still $46.9^{+8.7}_{-8.4}$% even when only AGNs with $L_X > 10^{43}$ erg s^{-1} are considered. Furthermore, the fraction of hosts in the *Disturbed I* and *Disturbed II* categories are $18.8^{+8.7}_{-5.0}$% and $53.1^{+8.4}_{-8.8}$%, respectively, and in rough agreement with the percentages found for the full sample.

6. DISCUSSION

In summary, our primary findings are as follows: (1) moderate luminosity, X-ray-selected AGNs at $z \sim 2$ do not exhibit a significant excess of distorted morphologies relative to a mass-matched control sample at the same redshift; (2) both samples are dominated by systems that appear relatively relaxed and undisturbed, to the depth of our imaging; and (3) a large fraction ($51.4^{+5.8}_{-5.9}$%) of the AGNs reside in galaxies with discernible disks. Therefore, based on our visual classifications, we do not find a strong connection between highly disruptive major mergers and moderate luminosity AGN activity at $z \sim 2$.

If mergers play an important role in triggering AGN activity, there are two possible effects that have been discussed in the literature which could help explain the lack of disturbed morphologies among the AGN hosts. The first is obscuration; if obscured AGNs are preferentially associated with mergers, they may be systematically missed by X-ray surveys. It is well known that, in the local universe, gas-rich mergers have extremely high dust column densities, which may be sufficient to hide even hard X-ray sources deep in the nuclei (Hopkins et al. 2007). The second is a time delay between the onset of AGN activity and the actual merger. If this delay is of the same order as the relaxation time of the galaxy (typically $\sim$ few 100 Myr), the most obvious signatures of morphological disturbance will have faded by the time it is identified as an X-ray bright AGN (Lotz et al. 2010). Hydrodynamic simulations of SMBH growth in galaxy mergers do predict such a delay (Hopkins et al. 2006b), and there is observational evidence for a delay of the order of $\sim$250 Myr between starburst and AGN activity (Wild et al. 2010).

While these two effects can help explain the lack of obvious merger signatures among the AGN hosts, the high disk fraction we observe is harder to reconcile with the merger picture of AGN fueling. This finding that disk-like morphologies are prevalent among active galaxies at this redshift agrees with the recent findings of Schawinski et al. (2011), who examined a smaller sample of AGNs at $z \sim 2$ in the ERS region of GOODS-South. This characteristic does not appear to be limited to the AGN hosts, though, as we find disks are common among all massive galaxies at this redshift, regardless of whether they host an active nucleus. Nevertheless, the morphology of these galaxies provides an important clue to the mechanism that triggered their current AGN activity. It is doubtful that the disk-like structure of these galaxies could have survived the large scale and violent torquing of gas that occurs during a *major* galaxy–galaxy interaction (e.g., Bournaud et al. 2011a), making it highly unlikely that their nuclear activity is being fueled by a major merger-driven process. It is more likely that the nuclear activity in these disk galaxies is being fueled by the stochastic accretion of cold gas, possibly triggered by a disk instability or minor interaction that did not substantially perturb the large-scale structure of the galaxy.

Despite the prevalence of disk-like morphologies, we also find that the AGNs are more often associated with spheroids than their non-active counterparts. While the connection between spheroid-dominated galaxies and AGNs has been well established at lower redshifts, this is the first such finding at $z \sim 2$, where there is evidence that the canonical mass–morphology relationship appears to break down (McGrath et al. 2008; van der Wel et al. 2011). Even in an era where massive galaxies predominately have disk-like morphologies, our observations suggest SMBH continue to be preferentially embedded in spheroidal systems.

At higher X-ray luminosities ($L_X > 10^{43}$ erg s^{-1}) we also observe a shift in the overall AGN host population toward spheroids. Although many of these galaxies appear undisturbed, they may have been triggered by a merger event in the recent past and have since sufficiently relaxed. In the evolutionary sequence of a merger-triggered QSO presented in Hopkins et al. (2007), these systems would be in the post-blowout phase, when nuclear activity and X-ray luminosity are in gradual decline.

Our finding that more luminous AGNs are more often associated with spheroids generally agrees with the luminosity- and redshift-dependent AGN fueling model presented by Hopkins & Hernquist (2006; hereafter HH06), which proposes that luminous AGNs and QSOs are largely triggered by major mergers, while lower luminosity AGNs are fueled by the random accretion of gas via internal, secular processes. However, this model also predicts that by $z \sim 2$ the active galaxy population should be dominated by merger-triggered AGNs, even at moderate luminosities ($L_X \sim 10^{43}$ erg s^{-1}). This is because merger-driven accretion in this model is tied to the cosmological galaxy merger rate, which increases rapidly with redshift (Conselice et al. 2003; Kartaltepe et al. 2007) whereas quiescent accretion is related to the mass function and gas fraction of late-type galaxies, which evolve more slowly.

The HH06 model predicts that at $z = 2$ the number density of quiescently accreting AGNs will not equal that of merger-fueled AGNs until roughly *two orders of magnitude* below the knee in the AGN luminosity function. In the hard X-ray band this knee occurs at a luminosity of roughly $L_X \sim 10^{44}$ erg s^{-1} (Aird et al. 2010). This means the predicted X-ray luminosity at which an equal fraction of AGNs are fueled by quiescent and merger-triggered accretion at $z = 2$ is roughly $L_X \sim 10^{42}$ erg s^{-1}. If we assume that disk-like hosts are fueling their AGNs via internal processes and have not experienced a major merger in the recent past, then this prediction is at odds with the high disk fraction we observe at $L_X \sim 10^{43}$ erg s^{-1}, an order of magnitude above this luminosity. We find that the luminosity at which an equal fraction of AGNs are hosted by disk and spheroid galaxies is roughly $L_X \sim 10^{43}$ erg s^{-1}. This finding suggests that the stochastic fueling of SMBHs is far more prevalent at moderate luminosities than predicted by the HH06 model.

This apparent disagreement with the HH06 fueling model was previously reported at lower redshifts by Georgakakis et al. (2009), who found that the contribution to the X-ray luminosity function at $z \sim 1$ from AGNs in late-type hosts exceeded the predicted luminosity function for stochastically fueled AGNs. It was also noted by Cisternas et al. (2011), who found a large fraction (55.6%) of luminous AGNs ($L_X > 10^{44}$ erg s^{-1}) at $z \sim 1$ hosted by disk-dominated galaxies. While the high disk fraction we observe is similar to what has been previously reported in these studies, the disagreement between our findings and the predictions of the HH06 model is more acute given the higher redshift of our sample and the strong redshift evolution predicted for merger-driven accretion.

Overall our findings generally agree with an emerging consensus that major galaxy mergers likely play a subdominant role in triggering moderate-luminosity AGNs. This has been asserted from a morphological standpoint by Cisternas et al. (2011) and Georgakakis et al. (2009) at $z \sim 1$, and by Schawinski et al. (2011) at $z \sim 2$, based on the large disk fraction found among AGN hosts. It has also been proposed by Mullaney et al. (2011) based on the average specific star formation rates (SSFR) of AGN hosts out to $z \sim 3$. They find that a vast

majority of hosts have SSFRs consistent with the star-forming main sequence (Noeske et al. 2007) and that less than 10% appear to be undergoing a starburst phase. From this they conclude that the nuclear activity in these galaxies is being fueled by internal mechanisms rather than violent mergers. A similar conclusion was also reached by Allevato et al. (2011) based on the projected clustering of AGNs in the COSMOS field out to $z \sim 2.2$.

There are several reasons why non-merger related accretion may contribute more to the onset of AGN activity at this redshift than previously expected. This includes such things as a shorter post-blowout quasar lifetime, which would reduce the contribution from merger-triggered AGN to the X-ray luminosity function, or a faster evolving gas fraction than that assumed by HH06. It may also be due to the rise of violent gravitational instabilities in disk galaxies due to the effects of rapid cold flow accretion (Dekel et al. 2009). Such instabilities become increasingly common at $z > 1$ (Elmegreen et al. 2005; Genzel et al. 2006) and are not accounted for in the HH06 model. Unlike the weaker disk instabilities that are associated with secular evolution at low redshift (e.g., bar instabilities), these high-redshift instabilities are highly efficient at continuously funneling gas and stars to the centers of galaxies on short timescales (a single disk rotation) and at high inflow rates ($\sim 10\, M_{\odot}$ yr^{-1}; M. Cacciato et al. 2011, in preparation; Bournaud et al. 2011b), potentially fueling increased AGN activity in disk galaxies without the need for galaxy–galaxy mergers (Bournaud et al. 2011b).

Of course, the disagreement between the high disk fraction we observe and the merger-dominated fueling model is predicated on the assumption that disk-like hosts have not experienced a merger in the recent past. The two can be reconciled if these disks have instead survived or reformed following a merger event. Numerical simulations have shown that disks can reform after a merger if the interacting systems are gas-rich (Robertson et al. 2006; Bundy et al. 2010), although it has been argued that such interactions are not conducive to the fueling of SMBHs (Hopkins & Hernquist 2009). Alternatively, minor mergers provide a means to trigger AGN activity within galaxies without entirely destroying their preexisting morphology. Semi-analytic cosmological galaxy formation models in which all AGN activity is assumed to be triggered by mergers (Somerville et al. 2008) do predict that the average merger event that triggers an AGN with $L_X > 10^{42}$ erg s^{-1} has a mass ratio of 1:8 as opposed to the more disruptive 1:1 or 1:2 mergers (R. S. Somerville et al. 2011, in preparation). Coupled with a time delay between the merger and the visibility of the AGN, the signatures of these mergers could prove difficult to detect. Therefore, since we cannot rule out such interactions, minor mergers would seem to be one of the remaining ways to reconcile the merger-dominated fueling model with the high disk fraction and lack of disturbed morphologies that we observe.

7. CONCLUSIONS

To explore whether major galaxy mergers are the primary mechanism fueling AGN activity at $z \sim 2$, we have used *HST*/WFC3 imaging to examine the rest-frame optical morphologies of galaxies hosting moderate-luminosity, X-ray-selected AGNs at $z = 1.5$–2.5. Employing visual classifications, we have determined both the predominant morphological type of these galaxies and the frequency at which they exhibit morphological disturbances indicative of recent interactions. To determine whether the AGN hosts show merger or interaction signatures more often than similar non-active galaxies, we have also classified a sample of mass-matched control galaxies at the same redshift.

First, we find that just over half of the AGNs reside in disk galaxies ($51.4^{+5.8}_{-5.9}$%), while a smaller percentage are found in spheroids ($27.8^{+5.8}_{-4.6}$%) and systems with irregular morphologies ($16.7^{+5.3}_{-3.5}$%). This high disk fraction is also observed among the control galaxies ($69.0^{+2.9}_{-3.3}$% of which are disks), which indicates that disk-like morphologies are prevalent among all massive galaxies at this redshift, regardless of whether they host an active nucleus. In fact, we find the AGNs to be more often associated with spheroidal galaxies compared to their non-active counterparts. Pure spheroids account for $27.8^{+5.8}_{-4.6}$% of the active galaxies, while comprising only $16.9^{+2.8}_{-2.2}$% of the control galaxies. At X-ray luminosities above 10^{43} erg s^{-1} we observe a reversal in the morphological make-up of the AGN hosts, with spheroids and disks comprising $40.6^{+9.0}_{-7.9}$% and $34.4^{+9.1}_{-7.3}$% of the sample, respectively.

Second, we find that $16.7^{+5.3}_{-3.5}$% of the AGN hosts have highly disturbed morphologies and appear to be involved in a major merger or interaction, while $44.4^{+5.9}_{-5.6}$% show at least some disturbance, including minor asymmetries in their morphologies. In both cases, these fractions are statistically consistent with the fraction of control galaxies that show similar morphological disturbances. Most galaxies in both the control and AGN samples appear relatively relaxed and undisturbed, to the depth of our imaging ($55.6^{+5.6}_{-5.9}$% and $52.1^{+3.3}_{-3.4}$%, respectively). These results suggest that the AGN hosts are no more likely to be involved in an ongoing major merger or interaction than non-active galaxies of similar mass.

Finally, the high disk fraction observed among the AGN hosts appears to be at odds with predictions that major merger-driven accretion should be the dominant AGN fueling mode at $z \sim 2$. The presence of a large population of relatively undisturbed disk-like hosts suggests that either secular evolution, disk instability-driven accretion, minor mergers, or a combination of the three, play a greater role in triggering AGN activity at these redshifts than previously thought. In a forthcoming paper we plan to calculate the fraction of the AGN X-ray luminosity function attributable to these disk-hosted AGNs in order to quantify any discrepancy between our observations and merger-triggered AGN fueling models.

Support for Program number HST-GO-12060 was provided by NASA through a grant from the Space Telescope Science Institute, which is operated by the Association of Universities for Research in Astronomy, Incorporated, under NASA contract NAS5-26555. Furthermore, D.K. is funded in part by the NSF under grant No. AST-0808133.

REFERENCES

Aird, J., Nandra, K., Laird, E. S., et al. 2010, MNRAS, 401, 2531
Allevato, V., Finoguenov, A., Cappelluti, N., et al. 2011, ApJ, 736, 99
Barger, A. J., & Cowie, L. L. 2005, ApJ, 635, 115
Barnes, J. E., & Hernquist, L. E. 1991, ApJ, 370, L65
Bauer, F. E., Alexander, D. M., Brandt, W. N., et al. 2002, AJ, 124, 2351
Bennert, N., Canalizo, G., Jungwiert, B., et al. 2008, ApJ, 677, 846
Bertin, E., & Arnouts, S. 1996, A&AS, 117, 393
Bournaud, F., Chapon, D., Teyssier, R., et al. 2011a, ApJ, 730, 4
Bournaud, F., Dekel, A., Teyssier, R., et al. 2011b, ApJL, in press, (arxiv:1107.1483)
Brusa, M., Comastri, A., Daddi, E., et al. 2005, A&A, 432, 69
Bruzual, G., & Charlot, S. 2003, MNRAS, 344, 1000
Bundy, K., Georgakakis, A., Nandra, K., et al. 2008, ApJ, 681, 931

Bundy, K., Scarlata, C., Carollo, C. M., et al. 2010, ApJ, 719, 1969
Cameron, E. 2011, PASA, 28, 128
Canalizo, G., & Stockton, A. 2001, ApJ, 555, 719
Cisternas, M., Jahnke, K., Inskip, K. J., et al. 2011, ApJ, 726, 57
Conselice, C. J., Bershady, M. A., Dickinson, M., & Papovich, C. 2003, AJ, 126, 1183
Davis, M., Guhathakurta, P., Konidaris, N. P., et al. 2007, ApJ, 660, L1
Dekel, A., Sari, R., & Ceverino, D. 2009, ApJ, 703, 785
de Vaucouleurs, G. 1948, Ann. Astrophys., 11, 247
Di Matteo, P., Combes, F., Melchior, A.-L., & Semelin, B. 2007, A&A, 468, 61
Dunlop, J. S., McLure, R. J., Kukula, M. J., et al. 2003, MNRAS, 340, 1095
Elmegreen, B. G., Elmegreen, D. M., Vollbach, D. R., Foster, E. R., & Ferguson, T. E. 2005, ApJ, 634, 101
Ferrarese, L., & Merritt, D. 2000, ApJ, 539, L9
Gabor, J. M., Impey, C. D., Jahnke, K., et al. 2009, ApJ, 691, 705
Garmire, G. P., Bautz, M. W., Ford, P. G., Nousek, J. A., & Ricker, G. R., Jr. 2003, Proc. SPIE, 4851, 28
Gawiser, E., van Dokkum, P. G., Herrera, D., et al. 2006, ApJS, 162, 1
Gebhardt, K., Bender, R., Bower, G., et al. 2000, ApJ, 539, L13
Genzel, R., Tacconi, L. J., Eisenhauer, F., et al. 2006, Nature, 442, 786
Georgakakis, A., Coil, A. L., Laird, E. S., et al. 2009, MNRAS, 397, 623
Giavalisco, M., Ferguson, H. C., Koekemoer, A. M., et al. 2004, ApJ, 600, L93
Grogin, N. A., Conselice, C. J., Chatzichristou, E., et al. 2005, ApJ, 627, L97
Grogin, N. A., Kocevski, D. D., Faber, S. M., et al. 2011, arXiv:1105.3753
Häring, N., & Rix, H.-W. 2004, ApJ, 604, L89
Hopkins, P. F., Bundy, K., Hernquist, L., & Ellis, R. S. 2007, ApJ, 659, 976
Hopkins, P. F., & Hernquist, L. 2006, ApJS, 166, 1
Hopkins, P. F., & Hernquist, L. 2009, ApJ, 694, 599
Hopkins, P. F., Hernquist, L., Cox, T. J., & Kereš, D. 2008, ApJS, 175, 356
Hopkins, P. F., Hernquist, L., Cox, T. J., et al. 2005, ApJ, 630, 716
Hopkins, P. F., Hernquist, L., Cox, T. J., Robertson, B., & Springel, V. 2006a, ApJS, 163, 50
Hopkins, P. F., Hernquist, L., Cox, T. J., et al. 2006b, ApJ, 639, 700
Jahnke, K., Sánchez, S. F., Wisotzki, L., et al. 2004, ApJ, 614, 568
Kartaltepe, J. S., Sanders, D. B., Le Floc'h, E., et al. 2010, ApJ, 721, 98
Kartaltepe, J. S., Sanders, D. B., Scoville, N. Z., et al. 2007, ApJS, 172, 320
Kauffmann, G., Heckman, T. M., Tremonti, C., et al. 2003, MNRAS, 346, 1055
Koekemoer, A. M., Faber, S. M., Ferguson, H. C., et al. 2011, arXiv:1105.3754
Koekemoer, A. M., Fruchter, A. S., Hook, R. N., & Hack, W. 2002, in The 2002 HST Calibration Workshop: Hubble after the Installation of the ACS and the NICMOS Cooling System, ed. S. Arribas, A. Koekemoer, & B. Whitmore (Baltimore, MD: STScI), 337
Laird, E. S., Nandra, K., Georgakakis, A., et al. 2009, ApJS, 180, 102
Lotz, J. M., Jonsson, P., Cox, T. J., & Primack, J. R. 2010, MNRAS, 404, 575
Luo, B., Bauer, F. E., Brandt, W. N., et al. 2008, ApJS, 179, 19
Magorrian, J., Tremaine, S., Richstone, D., et al. 1998, AJ, 115, 2285
Marconi, A., & Hunt, L. K. 2003, ApJ, 589, L21
McGrath, E. J., Stockton, A., Canalizo, G., Iye, M., & Maihara, T. 2008, ApJ, 682, 303
Mihos, J. C., & Hernquist, L. 1996, ApJ, 464, 641
Mullaney, J. R., Pannella, M., Daddi, E., et al. 2011, MNRAS, in press (arXiv:1106.4284)
Noeske, K. G., Weiner, B. J., Faber, S. M., et al. 2007, ApJ, 660, L43
Peng, C. Y., Ho, L. C., Impey, C. D., & Rix, H.-W. 2002, AJ, 124, 266
Pierce, C. M., Lotz, J. M., Laird, E. S., et al. 2007, ApJ, 660, L19
Robertson, B., Bullock, J. S., Cox, T. J., et al. 2006, ApJ, 645, 986
Sánchez, S. F., Jahnke, K., Wisotzki, L., et al. 2004, ApJ, 614, 586
Schawinski, K., Treister, E., Urry, C. M., et al. 2011, ApJ, 727, L31
Scoville, N., Aussel, H., Brusa, M., et al. 2007, ApJS, 172, 1
Sérsic, J. L. 1968, Atlas de galaxias australes (Cordoba, Argentina: Observatorio Astronomico)
Silverman, J. D., Mainieri, V., Salvato, M., et al. 2010, ApJS, 191, 124
Somerville, R. S., Hopkins, P. F., Cox, T. J., Robertson, B. E., & Hernquist, L. 2008, MNRAS, 391, 481
Stockton, A. 1982, ApJ, 257, 33
Sutherland, W., & Saunders, W. 1992, MNRAS, 259, 413
van der Wel, A., Rix, H.-W., Wuyts, S., et al. 2011, ApJ, 730, 38
Wild, V., Heckman, T., & Charlot, S. 2010, MNRAS, 405, 933
Windhorst, R. A., Cohen, S. H., Hathi, N. P., et al. 2011, ApJS, 193, 27
Wuyts, S., Labbé, I., Schreiber, N. M. F., et al. 2008, ApJ, 682, 985
Xue, Y. Q., Luo, B., Brandt, W. N., et al. 2011, ApJS, 195, 10